Journal of Simulation and Analysis of Novel Technologies in Mechanical Engineering
15 (1) (2023) 0005~0013

Research article

Dynamic model of static synchronous compensator in Single-Machine Infinite-Bus power system

Sayed Mohammadali Zanjani[1, 2]

[1]*Smart Microgrid Research Center, Najafabad Branch, Islamic Azad University, Najafabad, Iran*
[2]*Department of Electrical Engineering, Najafabad Branch, Islamic Azad University, Najafabad, Iran*

sma_zanjani@pel.iaun.ac.ir

(Manuscript Received --- 13 Jan. 2023; Revised --- 21 Feb. 2023; Accepted --- 25 Feb. 2023)

Abstract

Electric loads such as electric arc furnaces, and heavy industrial plants can produce or absorb reactive power. Due to the instantaneous change of loads, the reactive power balance is essential in a power system. Static synchronous compensator (STATCOM) is usually used to control the reactive power. By controlling the reactive power absorbed or injected into the power system, it makes the voltage at the point of connection to the grid. This compensator is used in two stable operating modes, inductive (lag) and capacitive (leading), to improve the performance of the power system. In this paper, a single-machine power system with shunt compensator is considered and the aim is to determine the relationship between voltage and current between the compensator and the transmission line. An approximate model is considered for the compensator, where the compensator current plays the main role. Then, using the analysis of algebraic equations, the voltage in the compensating bus was determined. Finally, the simulation results show the behavior of the compensator for different modes.

Keywords: Modelling, Shunt device, Static synchronous compensator

1- Introduction

The rapid development of power electronics and the construction of high-power semiconductors have provided amazing possibilities for the development of new equipment in the field of power system compensators [1,2]. So far, many control tools have been designed and completed under the name of flexible alternating current transmission systems (FACTS) technology for transmission and distribution networks [3, 4]. FACTS devices are divided into two groups based on the mode of operation, devices based on reactive impedance and devices based on voltage source [5,6]. In another division, flexible ac transmission systems are divided into three groups of thyristor-controlled FACTS devices, FACTS devices based on voltage source converters, and hybrid devices. In terms of connection type, FACTS controllers, according to Fig. 1 are divided into four types [7,8],

a) series controller such as thyristor controlled series capacitor (TCSC) [9,10] and synchronous static series compensator (SSSC) [11,12], b) shunt controller such as static variable compensator (SVC) [13,14] and static synchronous compensator (STATCOM) [15,16], c) series-series controller such as inter-line power flow controller (IPFC) [17,18] and adjustment thyristor controlled phase angle controller (TCPAR) [19] and d) series-parallel controller such as uniform power distribution controller (UPFC) are divided [20,21].

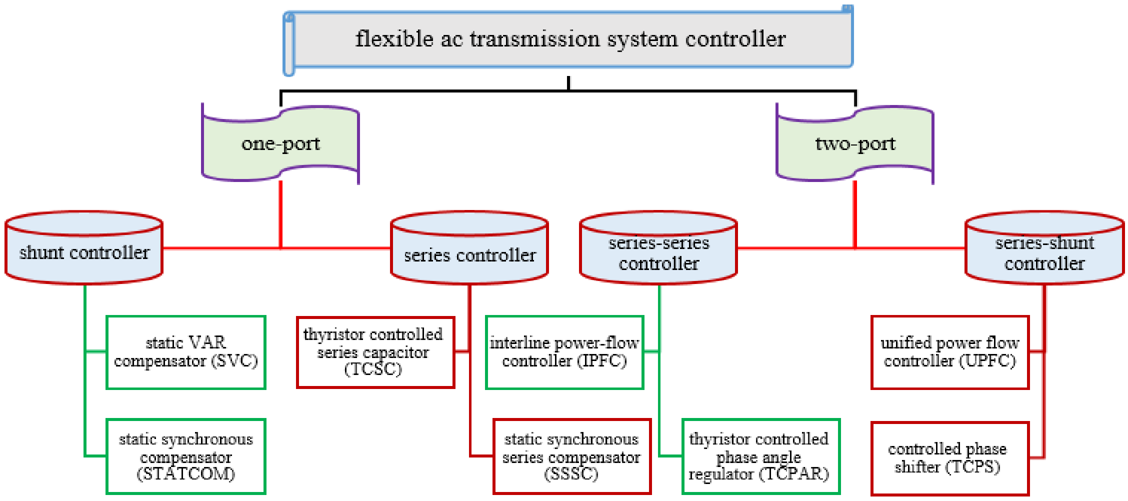

Fig. 1 Classification of FACTS devices

From the use of FACTS devices, we can mention the control of load distribution and minimizing the losses of transmission lines, increasing dynamic stability, strengthening transient stability, reliability or security, improving power quality and improving voltage profile [22,23,24].

Various studies have been presented on the application of STATCOM to improve the performance of power systems, such as ferroresonance overvoltage mitigation in grid-connected wind energy conversion systems [25], mitigate resonance in wind farms [26], power oscillation damping in PV solar system [27], reactive power compensation [28] and transient stability enhancement in distribution system with wind farms [29].

A static synchronous compensator along with a variable frequency drive for voltage and frequency control of a small-hydro turbine driven self-excited induction generator system is proposed in [30], in which a control algorithm based on adaptive noise cancellation filter is used for STATCOM control.

A comprehensive review of various techniques employed to enhance the low voltage ride-through capability of the fixed-speed induction generators- based wind turbines is presented in [31], which, based on the simulated results, series connection dynamic voltage restorer and shunt connection static synchronous compensators are the highly efficient low voltage ride through capability enhancement approaches.

To control the controllers and clarify the objectives, the nonlinear controller is proposed in [32] as an alternative to the traditional STATCOM controller in a wind farm equipped with a double-fed induction generator (DFIG). So that the reactive power required to stabilize the wind farm equipped with DFIG is considered when a fault occurs.

The integration of a STATCOM in a wind park (WP)-based DFIG is presented in [33], and the effect of the STATCOM on the high voltage ride-through (HVRT) capability of the WP is analyzed. In this study, the size of the STATCOM is selected based on the network code to control the power factor and different wind turbine and medium voltage feeder outage scenarios. Finally, the simulation results show the use of STATCOM to significantly improve the HVRT WP capability.

This paper presents the single-machine infinite-bus (SMIB) power system model with a compensator. In this model, the compensator is represented by a current source. The algebraic equations of the power system have been analyzed by ignoring the resistance of the transmission line. The simulation results are obtained and shown in MATLAB software using equations.

2- Static Synchronous Compensator

The static synchronous compensator is a power electronic converter designed to be shunt-connected with the grid to compensate for reactive power [34, 35].

STATCOM has the following components: A voltage source converter (VSC), dc capacitor, inductive reactance and harmonic filter [36]. By controlling the reactive power absorbed or injected into the power system through the VSC, the STATCOM performs voltage regulation at its connection point [37, 38]. Harmonic filter attenuates the harmonics and other high frequency components due to the VSC [39,40]. A simplified diagram of STATCOM is shown in Fig. 2. The operation of STATCOM can be classified into two modes: voltage regulation mode and VAR control mode (Fig. 3).

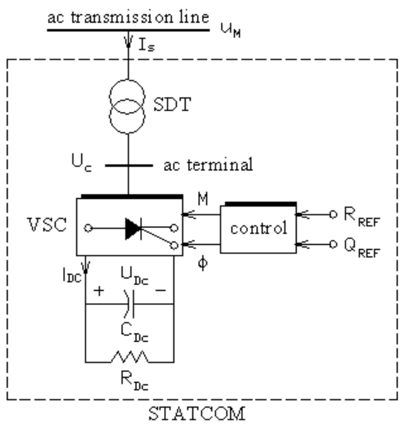

Fig. 2 Compensator structure schematic

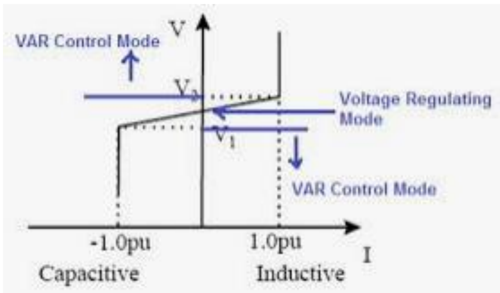

Fig. 3 Compensating performance area

3- Power System with Compensator

A single-machine system connected to an infinite bus with shunt compensator is shown in Fig. 4, where the generator bus voltage is U_T, the infinite bus voltage is U_B and the compensating bus voltage is U_M. Also, the terminal current of the generator I_T and compensating current I_S being considered. The length of the line is “a” and “λ” is a parameter between 0 and 1, and it represents the ratio of the compensator distance from the generator terminal to the total length of the line. The impedance between the generator bus and the compensator bus and the compensator bus with the infinite bus are respectively based on the location of the compensator regardless of the capacitance of the transmission line R_1+jX_1 and R_2+jX_2.

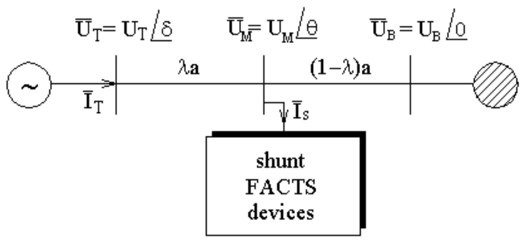

Fig. 4 Single-machine system connected to infinite bus with shunt compensator

4- System Equations

The compensating equivalent circuit is considered equivalent to the controllable reactive current source according to Fig. 5. The output current can be controlled separately in both capacitive and capacitive ranges. According to the voltage converter in the compensator, the compensator current is post-phase or pre-phase Due to the bus voltage.

Based on the relationship between voltage (KVL) and current (KCL) in the transmission line, the compensating bus voltage is:

$$\bar{U}_M = \frac{X_2}{X_T}\bar{U}_T + j\frac{X_1X_2}{X_T}\bar{I}_S + \frac{X_1}{X_T}\bar{U}_B \tag{1}$$

In the following, the analysis of system equations is expressed in two frameworks, and the compensatory behavior is simulated using it.

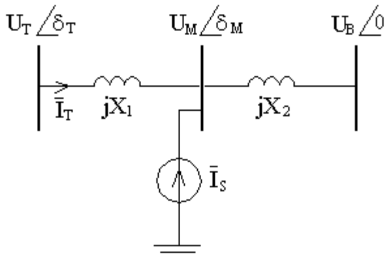

Fig. 5 Compensating equivalent circuit in power system transmission line

A- Analysis in two-axis dq framework

The angle between compensating bus voltage and "q" axis is considered θ.

i_{sd} and i_{sq} are the compensating current components and U_{Bd} and U_{Bq} are compensating bus voltage components in dq axis framework.

a) Generator terminal current components

According to the relationship between generator terminal voltage components u_d and u_q and generator terminal current components i_d and i_q, and also according to the definition of biaxial components of infinite bus voltage and compensating current, the terminal current components Generators include:

$$\begin{cases} i_d = \dfrac{E_q^{'} - X_2 I_S \cos\theta - U_B \cos\delta}{X_1 + X_2 + X_d^{'}} \\ i_q = \dfrac{X_2 I_S \sin\theta + U_B \sin\delta}{X_1 + X_2 + X_q} \end{cases} \tag{2}$$

b) Compensating bus voltage components

Using the generator terminal current components, we have:

$$\begin{cases} U_{Md} = \dfrac{(X_1 + X_q) U_B \sin\delta + (X_1 + X_q) X_2 I_S \sin\theta}{X_1 + X_2 + X_q} \\ U_{Mq} = \dfrac{X_2 E_q^{'} + (X_1 + X_d^{'}) U_B \cos\delta + (X_1 + X_d^{'}) X_2 I_S \cos\theta}{X_1 + X_2 + X_d^{'}} \end{cases} \tag{3}$$

c) Compensating bus voltage angle

Using compensating bus voltage components in dq biaxial device, we have:

$$tg\theta = \frac{U_{Md}}{U_{Mq}} = \frac{X_1 + X_2 + X_d^{'}}{X_1 + X_2 + X_q} \frac{(X_1 + X_q)(U_B \sin\delta + X_2 I_S \sin\theta)}{X_2 E_q^{'} + (X_1 + X_d^{'})(U_B \cos\delta + X_2 I_S \cos\theta)} \tag{4}$$

d) Active power of the generator

Based on the definition of the mixed power of the generator, the active power is equal to:

$$P_E = \frac{U_M^2}{2} \frac{X_d^{'} - X_q}{(X_1 + X_d^{'})(X_1 + X_q)} \sin 2\theta + \frac{E_q^{'} U_M}{(X_1 + X_d^{'})} \sin\theta \tag{5}$$

B- Analysis in two-axis xy framework

The compensating reactive current in capacitive mode is:

$$\bar{I}_S = I_S e^{j(\delta_M - 90)} \quad (6)$$

So the components are:

$$\begin{cases} i_{Sx} = I_S \sin\delta_M \\ i_{Sy} = I_S \cos\delta_M \end{cases} \quad (7)$$

a) voltage magnitude of compensating bus

The magnitude of compensating bus voltage components is:

$$\begin{cases} U_{Mx} = \frac{X_2}{X_T} U_x + \frac{X_1 X_2}{X_T} I_S \cos\delta_M + \frac{X_1}{X_T} U_B \\ U_{My} = \frac{X_2}{X_T} U_y + \frac{X_1 X_2}{X_T} I_S \sin\delta_M \end{cases} \quad (8)$$

Therefore, the magnitude and phase of the compensating bus voltage is equal to:

$$\delta_M = tg^{-1}\left(\frac{X_2 U_T \sin\delta_T}{X_2 U_T \cos\delta_T + X_1 U_B}\right) \quad (9)$$

$$U_M = \frac{X_1 X_2 I_S + X_2 U_T \cos(\delta_T - \delta_M) + X_1 U_B \cos\delta_M}{X_T} \quad (10)$$

As found, the compensating current has an effect on the magnitude and phase of the compensating bus voltage. The magnitude of the compensating bus voltage can be expressed as follows:

$$U_M = \frac{1}{X_T}\sqrt{(X_1 U_B)^2 + (X_2 U_T)^2 + 2 X_1 X_2 U_T U_B \cos\delta_T} + \frac{X_1 X_2}{X_T} I_S \quad (11)$$

The first component is the bus voltage M without the compensating effect, and the second component shows the compensating effect on the voltage magnitude.

b) Voltage angle of the generator bus

According to the voltage components of the generator terminal in the xy framework, the voltage angle in the generator bus is equal to:

$$\delta_T = tg^{-1}\left[\frac{[X_T U_M - X_1 X_2 I_S]\sin\delta_M}{[X_T U_M - X_1 X_2 I_S]\cos\delta_M - X_1 U_B}\right] \quad (12)$$

c) Generator Active and reactive powers

Based on the mixed power in the terminal bus of the generator, the active and reactive powers of the generator are equal to:

$$P_E = \frac{U_T U_B}{X_T}\sin(\delta_T) + \frac{X_2 U_T}{X_T} I_S \sin(\delta_T - \delta_M) \quad (13)$$

$$Q_E = \frac{U_T^2}{X_T} - \frac{U_T U_B}{X_T}\cos\delta_T - \frac{X_2 U_T}{X_T} I_S \cos(\delta_T - \delta_M) \quad (14)$$

Therefore, the active power consists of two components, the first component is related to the time when there is no compensator, and the second component shows the effect of the compensator, which is a function of the compensator current.

d) Compensating bus voltage angle

The compensating bus voltage phase can be determined according to the output power. Because the transmission line losses are zero, the active power produced by the generator is equal to the active power delivered to the infinite bus. The phase angle of the compensating bus voltage is independent of the compensating current, and the compensating current cannot change the voltage angle in the M bus. The compensating bus angle is:

$$\delta_M = tg^{-1}\left(\frac{X_2 U_T \sin\delta_T}{X_2 U_T \cos\delta_T + X_1 U_B}\right) \quad (15)$$

5- Simulation results

In this section, based on the relationships expressed in MATLAB software, the simulation results of compensatory behavior are presented.

Figs. 6 and 7 show the changes in active and reactive power at the generator terminal.

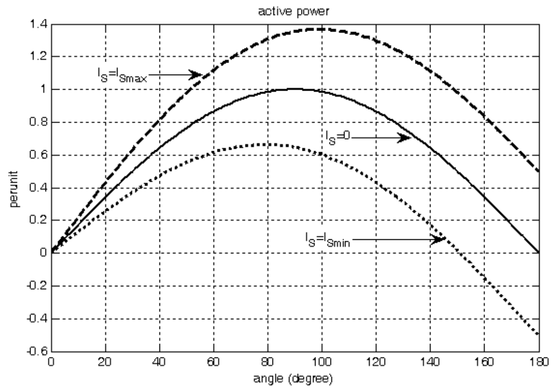

Fig. 6 Active power changes at the generator terminal according to the voltage angle of the generator terminal

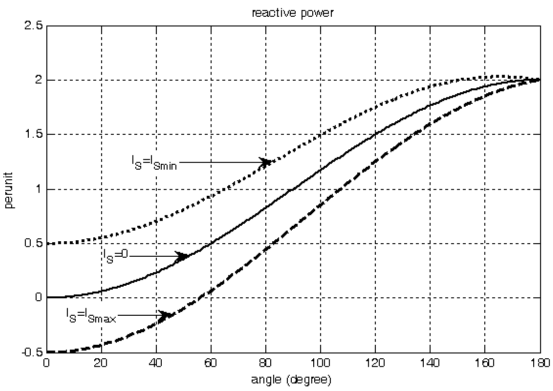

Fig. 7 Reactive power changes at the generator terminal according to the voltage angle of the generator terminal

Figs. 8 and 9 show changes in compensating bus voltage and compensating reactive power according to the generator terminal voltage angle. The above results have been obtained for three cases without compensator (zero compensator current is assumed), maximum and minimum compensator current.

The simulation results show that in the maximum state of the compensating current, the maximum active power value has increased, and it improves the system's stability against possible changes. Fig. 10 shows the effect of compensating current on compensating output power.

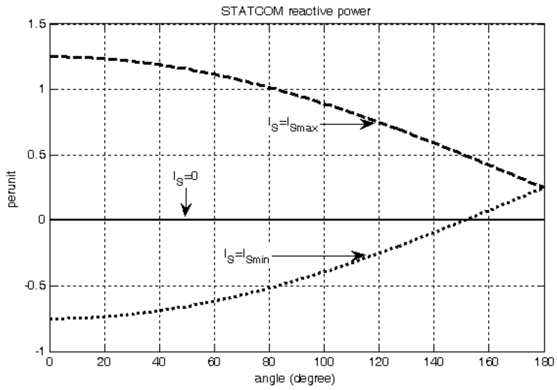

Fig. 8 Compensatory reactive power changes according to generator terminal voltage angle

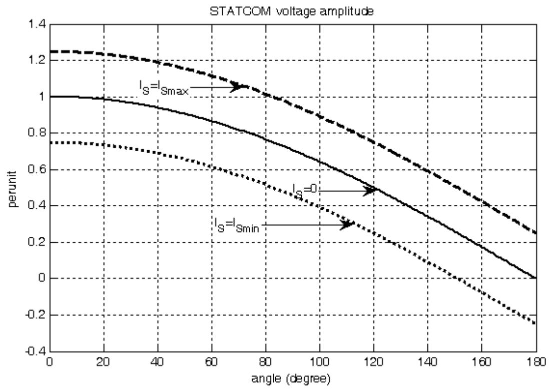

Fig. 9 Variations of compensating bus voltage according to generator terminal voltage angle

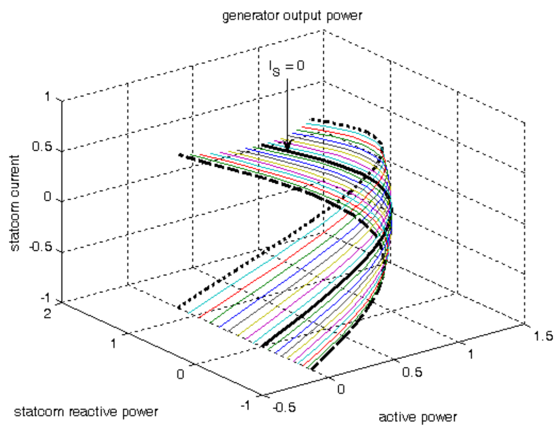

Fig. 10 Effect of compensating current on output power

6- Conclusion

Using STATCOM at the appropriate point or points in the power system improves the ability to transfer power to loads, which is done in different network conditions by increasing voltage stability and setting a smooth voltage profile.

This paper presents the power system model equipped with a compensator. Then, using the analysis of algebraic equations in two devices, voltage and current changes and electric power, have been shown. As the results show, the system characteristics can be improved with the current source controlled by the compensator.

References

[1] Joseph, T., Ugalde-Loo, C.E., Liang, J., Coventry, P.F. (2018). Asset Management Strategies for Power Electronic Converters in Transmission Networks: Application to Hvdc and FACTS Devices. *IEEE Access*, 6, 21084-21102.

[2] Shahgholian, G. (2023). A brief overview of microgrid performance improvements using distributed FACTS devices. *Journal of Renewable Energy and Environment*, 10(1), 43-58.

[3] Zanjani, S., Azimi, Z., Azimi, M. (2011). Assesment and analyze hybride control system in distribution static synchronous compensator based current source converter. *Journal of Intelligent Procedures in Electrical Technology*, 2(7), 59-67.

[4] Shahgholian, G., Hamidpour, H., Movahedi, A. (2018). Transient stability promotion by FACTS controller based on adaptive inertia weight particle swarm optimization method. *Advances in Electrical and Electronic Engineering*, 16(1), 57-70.

[5] Barani, A., Moazzami, M., Honarvar, M.A., Zanjani, S.M.A. (2022). Decentralized robust adaptive control based on dynamic programming for SVC complement controller design. *International Journal of Smart Electrical Engineering*, 11(1), 41-48.

[6] Shahgholian, G., Faiz, J. (2010). Static synchronous compensator for improving performance of power system: A review. *International Review of Electrical Engineering*, 4(2), 2333-2342.

[7] Shahgholian, G., Mardani, E., Fattollahi, A. (2017). Impact of PSS and STATCOM devices to the dynamic performance of a multi-machine power system, *Engineering, Technology and Applied Science Research*, 7(6), 2113-2117.

[8] Motaghi, A., AaLIzadeh, M., Abbasian, M. (2019). Reactive power compensation and reducing network transmission losses by optimal placement of parallel and series FACTS devices with fuzzy-evolutionary method. *Journal of Intelligent Procedures in Electrical Technology*, 9(35), 27-38.

[9] Fathollahi, A., Kargar, A., Derakhshandeh, S.Y. (2022). Enhancement of power system transient stability and voltage regulation performance with decentralized synergetic TCSC controller. *International Journal of Electrical Power and Energy Systems*, 135, 107533.

[10] Fattollahi, A. (2017). Simultaneous design and simulation of synergetic power system stabilizers and a thyristor-controller series capacitor in multi-machine power systems. *Journal of Intelligent Procedures in Electrical Technology*, 8(30), 3-14.

[11] Bhukya, J., Mahajan, V. (2019). Optimization of damping controller for PSS and SSSC to improve stability of interconnected system with DFIG based wind farm. *International Journal of Electrical Power and Energy Systems*, 108, 314-335.

[12] Rashad, A., Kamel, S., Jurado, F. (2018). Stability improvement of power systems connected with developed wind farms using SSSC controller. *Ain Shams Engineering Journal*, 9(4), 2767-2779.

[13] Čerňan, M., Müller, Z., Tlustý, J., Valouch, V. (2021). An improved SVC control for electric arc furnace voltage flicker mitigation. *International Journal of Electrical Power and Energy Systems*, 129, 106831.

[14] Shahgholian, G., Etesami, A., (2011). The effect of thyristor controlled series compensator on power system oscillation damping control. *International Review of Electrical Engineering*, 5(2), 1822-1830.

[15] Shahgholian, G., Fazeli-Nejad, S., Moazzami, M., Mahdavian, M. Azadeh, Janghorbani, M., Farazpey, S. (2016). Power system oscillations damping by optimal coordinated design between PSS and STATCOM using PSO and ABC algorithms. *Proceeding of the IEEE/ECTI-CON*, Chiang Mai, Thailand, 1-6.

[16] Chen, Y., He, J. (2023). Fault detection and ride through of CHB converter-based star-connected STATCOM through exploring the inherent information of multiloop controllers. *IEEE Trans. on Power Electronics*, 38(2), 1366-1371.

[17] Shahgholian, G., Mahdavian, M., Noorani-Kalteh, M. Janghorbani, M.R. (2014). Design of a new IPFC-based damping neurocontrol for enhancing stability of a power system using particle swarm optimization. *International Journal of Smart Electrical Engineering*, 3(2), 73-78.

[18] Mishra, A., Gundavarapu, V.N.K. (2016). Line utilisation factor-based optimal allocation of IPFC and sizing using firefly algorithm for congestion management. *IET Generation, Transmission and Distribution*, 10(1), 115-122.

[19] Basiri-Kejani, M., Gholipour, E. (2017). Holomorphic embedding load-flow modeling of thyristor-based FACTS controllers. *IEEE Trans. on Power Systems*, 32(6), 4871-4879.

[20] Gandhar, S., Ohri, J., Singh, M. (202). Dynamic reactive power optimization of hybrid micro grid in islanded mode using fuzzy tuned UPFC, *Journal of Information and Optimization Sciences*, 41(1).

[21] Nahak, N., Mallick, R.K. (2019). Investigation and damping of low-frequency oscillations of stochastic solar penetrated power system by optimal dual UPFC, *IET Renewable Power Generation*, 13(3), 376-388.

[22] Mahdavian, M., Janghorbani, M., Eshaghpour, I., Ganji, E. (2017). Analysis and simulation of UPFC in electrical power system for power flow control. *Proceeding of the IEEE/ECTI-CON*, 62-65, Phuket, Thailand.

[23] Shahgholian, G., Movahedi, A. (2011). Coordinated control of TCSC and SVC for system stability enhancement using ANFIS method. *International Review on Modelling and Simulations*, 4(5), 2367-2375.

[24] Farhang, S., Zanjani, S.M.A., Fani, B. (2022). Analysis and simulation of inverter-based microgrid droop control method in island operation mode. *Signal Processing and Renewable Energy*, 6(1), 65-81.

[25] Mosaad, M.I., Sabiha, N.A. (2022). Ferroresonance overvoltage mitigation using STATCOM for grid-connected wind energy conversion systems". *Journal of Modern Power Systems and Clean Energy*, 10(2), 407-415.

[26] Zhang, Y., Yang, Y., Chen, X., Gong, C. (2021). Intelligent parameter design-based impedance optimization of STATCOM to mitigate resonance in wind farms. *IEEE Journal of Emerging and Selected Topics in Power Electronics*, 9(3), 3201-3215.

[27] Varma, R.K., Maleki, H. (2019). PV solar system control as STATCOM (PV-STATCOM) for power oscillation damping, *IEEE Trans. on Sustainable Energy*, 10(4), 1793-1803.

[28] Qi, J., Zhao, W., Bian, X. (2020). Comparative study of SVC and STATCOM reactive power compensation for prosumer microgrids with DFIG-based wind farm integration. *IEEE Access*, 8, 209878-209885.

[29] Gounder, Y.K., Nanjundappan, D. Boominathan, V. (2016). Enhancement of transient stability of distribution system with SCIG and DFIG based wind farms using STATCOM. *IET Renewable Power Generation*, 2016(8), 1171-1180.

[30] Singh, B., Murthy, S.S., Chilipi, R.R., Madishetti, S., Bhuvaneswari, G. (2014). Static synchronous compensator-variable frequency drive for voltage and frequency control of small-hydro driven self-excited induction generators system, *IET Generation, Transmission and Distribution*, 8(9), 1528–1538.

[31] Moghadasi, A., Sarwat, A., Guerrero, J.M. (2016). A comprehensive review of low-voltage-ride-through methods for fixed-speed wind power generators. *Renewable and Sustainable Energy Reviews*, 55, 823-839.

[32] Shahgholian, G., Izadpanahi, N. (2016). Improving the performance of wind turbine equipped with DFIG using STATCOM based on input-output feedback linearization controller. *Energy Equipment and Systems*, 4(1), 65-79.

[33] Karaagac, U., Kocar, I., Mahseredjian, J., Cai, L., Javid, Z. (2021). STATCOM integration into a DFIG-based wind park for reactive power compensation and its impact on wind park high voltage ride-through capability. *Electric Power Systems Research*, 199, 107368.

[34] Shahgholian, G., Bayat, B. (2011). A new control technique for improving the oscillations and decreasing the harmonic components of voltage in STATCOM. *International Review of Electrical Engineering*, 6(6), 3163-3174.

[35] Jabbari, M., Mahdavian, M., Attarpour E., Leilaeyoun, A. (2011). Modeling and dynamic analysis of a STATCOM for system damping enhancement. *Proceeding of the IEEE/ISIE*, Gdansk, Poland, 1087-1092.

[36] Li, S., Xu, L., Haskew, T.A. (2013). Control of VSC-based STATCOM using conventional and direct-current vector control strategies. *International Journal of Electrical Power and Energy Systems*. 45(1), 175-186.

[37] Alskran, F., Simões, M.G. (2021) Multilevel current source converter-based STATCOM suitable for medium-voltage applications. *IEEE Trans. on Power Delivery* 36(2), 1222-1232.

[38] Haghighatdar-Fesharaki, F., Haghshenas, A. (2019). STATCOM controller design with using of improved robust backstepping algorithm based on PSO to reduce large signal disturbances in power systems. *Journal of*

Intelligent Procedures in Electrical Technology, 10(37), 3-12.

[39] Alilou, M., Sadi, S., Zamanian, S., Gholami, J., Moshari, S. (2021). Improving the efficiency of actual distribution system by allocating multi-DG and DSTATCOM. *Journal of Intelligent Procedures in Electrical Technology*, 12(45), 1-15.

[40] Zanjani, M.A., Eshtehardiha, S. (2007). Gain tuning PID and IP controller with an adaptive controller based on the genetic algorithm for improvement operation of STATCOM. *Proceeding of the WSEAS/ICEEPS-HV-EM*, 28-33, Venice, Italy.

[41] Mahdavian, M. (2010). State space analysis of power system stability enhancement with used the STATCOM. *Proceeding of the IEEE/ECTI-CON*, 1201-1205, Chiang Mai, Thailand.